www.czasopisma.pan.pl www.journals.pan.pl
Chemical and Process Engineering 2017, 38 (3), 363-377
DOI: 10.1515/cpe-2017-0028

# PYROLYSIS OF WASTE TYRES – THE EFFECT OF REACTION KINETICS ON THE RESULTS OF THERMOGRAVIMETRIC ANALYSIS

Robert Cherbański*[1], Krzysztof Wróblewski[2], Eugeniusz Molga[1]

[1]Warsaw University of Technology, Faculty of Chemical and Process Engineering, ul. Waryńskiego 1, Warsaw, Poland

[2]CONTEC Ltd., ul. Książęca 17/1B, Warsaw, Poland

This paper presents a systematic thermogravimetric (TG) study on the kinetics of end-of-life tyre (ELT) pyrolysis. In the experimental part of this work, TG results are compared for tyre samples of different mass and size. This shows that the conduction resistance in the milligram scale (up to ~100 mg) tyre sample can be neglected. A comparison of experimental results demonstrates that the characteristic maxima on the DTG curve (the first derivative of TG signal) shift towards higher temperatures for higher heating rates. This phenomenon is explained to have kinetic origin and it is not caused by the internal heat transfer resistance. In the modelling part of this work, the kinetic parameters of the Three-Component Simulation Model (TCSM) are calculated and compared to the literature values. Testing of the kinetic model is carried out using experiments with a varying heating rate. This shows the limitation of the simplified kinetic approach and the appropriate selection method of the kinetic parameters.

**Keywords:** TGA, pyrolysis, end-of-life tyres, kinetics, TCSM

## 1. INTRODUCTION

Approximately 3.6 million tonnes of used tyres were generated in Europe in 2013 (ETRMA, 2015). In general, used tyres can be divided into two groups: part-worn tyres and end-of-life tyres (ELTs). While part-worn tyres can be reused after retreading, end-of-life tyres can not be used on vehicles any more.

ELTs are classified as non-hazardous waste (Council Directive 91/156/EEC). However, potential hazards were identified for ELTs when landfilled. They mainly include landfill fires with emissions of toxic gases and leaching into water. Therefore, the direct disposal of ELTs in landfills is banned in Europe (Council Directive 1999/31/EC). Instead, the two following recovery routes of ELTs exist: material recovery and energy recovery.

Since ELTs have a similar calorific value as a high quality coal, they are used as a substitute to fossil fuels. The cement sector is the main application for energy recovery where ELTs are co-incinerated in cement kilns. Concerning material recovery ELTs are used in different civil engineering applications (e.g.: a foundation for roads and railways, coastal protection, insulation) and product applications (e.g.: children's playgrounds, sport fields, artificial turf).Tyre pyrolysis is an alternative to the above mentioned methods but for some technical and economic reasons it is applied at a limited scale in Europe. Pyrolysis is the thermal degradation of organic compounds which is carried out in the absence of oxygen. Therefore, the emissions of NOx and SOx are lower for pyrolysis of tyres when compared to incineration. Three fractions of the product are obtained from pyrolysis: solid (char), liquid (oil) and gaseous (gas). Typical yield of the char is in the range of 38 - 40 wt.% (Williams, 2013). Selling prices

*Corresponding authors, e-mail: Robert.Cherbanski@pw.edu.pl

of such a primary product are rather low and subsequent physical or chemical activation of the char is needed to obtain the secondary product of relatively high market value. The non-condensable gas and pyrolysis oil can be directly used to heat the pyrolysis reactor. On the other hand, improvement of the economics is possible when you consider separation of the oil into valuable chemical compounds. It follows from different analyses that pyrolysis oil contains significant concentrations of chemical compounds such as benzene, toluene, xylenes, styrene and limonene. Separation of these species can give the secondary products of relatively high market value (Williams, 2013).

Thermogravimetric analysis (TGA) is a well established method of thermal analysis. The measuring principle is based on an accurate measurement of sample weight as a function of temperature or time in a strictly defined and controlled environment. Analysis results are usually presented as a TG curve representing the relative sample mass and a DTG curve (the corresponding first derivative of the TG signal) representing the process rate. TGA is widely used in research of all types of organic and inorganic solids and liquids, especially to determine their thermal stability, thermal degradation kinetics or catalysts activity.

TGA is also used to investigate the kinetics of ELT pyrolysis. Frequently, kinetic modeling relies on deconvolution of the DTG curve and determination of kinetic parameters for individual components. This approach was applied in two different kinetic models proposed by Leung and Wang (Leung and Wang, 1999): Three-Component Simulation Model (TCSM) and Three-Elastomer Simulation Model (TESM). The TCSM assumes that the kinetics of ELT pyrolysis can be modeled using three major components which decompose independently. Such compounds as oil, plasticizer, moisture and other specific additives are treated as the first component. The other two components are natural rubber (NR) and styrene-butadiene rubber (SBR) or polybutadiene rubber (BR) depending on the mixture used for the tyre production. The TESM assumes that the kinetics of ELTs pyrolysis can be modeled using the three elastomers NR, SBR and BR together with their respective oil components (six components in total). Many researchers (Al-Salem et al., 2009; Galvagno et al., 2007; González et al., 2001; Lah et al., 2013; Mui et al., 2010; Seidelt et al., 2006; Quek and Balasubramanian, 2009) have dealt with the kinetic modeling of ELTs pyrolysis after Leung and Wang (1999). The details can be found in an excellent review by Quek and Balasubramanian (2012).

A lot of effort has been taken to better understand the complex reaction mechanism for ELTs pyrolysis (Al-Salem et al., 2009; Chen et al., 2001; Islam et al., 2009). However, most of the papers have been devoted to simplified kinetic models (Quek and Balasubramanian, 2012). Indeed, they are frequently used for practical reasons. For instance, the CFD modelling of pyrolysis reactors requires reliable and computationally cheap kinetic models (Rudniak and Machniewski, 2016). This gap can be filled by simplified approaches which assume tree, four or five major components. Mui et al. performed calculations for three, four and five components showing the best fit for the five-component model (Mui et al., 2008). More recently, Lah et al. developed a model acknowledging reaction kinetics and the internal heat transfer resistance during ELTs pyrolysis (Lah et al., 2013). The model was based on the individual consideration of four major compounds: volatiles, NR, BR and SBR. Moreover, influence of three different fabrics and wire on the reaction kinetics was considered.

This paper presents a systematic TGA study on the kinetics of ELTs pyrolysis. The original contribution of this work is that it explains the origin of the observed phenomenon of shifting the local maxima on DTG curves in the direction of higher temperatures for higher heating rates. The phenomenon is explained on the basis of reaction kinetics rather than the internal heat transfer resistance. Moreover, the kinetic model is verified with experiments of varying heating rates. The testing shows the limitation of the simplified kinetic approach and the appropriate selection method of the kinetic parameters.

## 2. EXPERIMENTAL

All experiments were performed in a thermobalance TG 209 F1 Libra (Netzsch, Germany) equipped with a micro furnace and a precise ultra-microbalance. The micro furnace is made of high-performance ceramics. Its maximum temperature is 1100 K and heating rates are in the range of 0.001 - 200 K/min. The ultra-microbalance under thermostatic control provides resolution of 0.1 μg.

The conditions of all performed measurements are shown in Table 1.

Table 1. Conditions of the performed measurements

| No. | $m$ (mg) | Stage | $T_0$ (K) | $\beta$ (K/min) | $T_f$ (K) | $t_{isotherm.}$ (min) | $\dot{V}$ (ml/min) |
|---|---|---|---|---|---|---|---|
| 1 | 24.17 | I | 300 | 50 | 1073 | 20 | 40 |
| 2 | 92.66 | I | | 50 | | | |
| 3 | 35.15 | I | | 20 | | | |
| 4 | 25.89 | I | | 10 | | | |
| 5 | 86.84 | I | | 10 | | | |
| 6 | 23.45 | I | | 1 | | | |
| 7 | 25.47 | I | | 1 | | | |
| 8 | 50.91 | I | 300 | 12.7 | 672 | - | 40 |
| | | II | 672 | 3.33 | 773 | 4 | |
| 9 | 14.9 | I | 300 | 21.24 | 659 | - | 40 |
| | | II | 659 | 5.63 | 873 | 4 | |
| 10 | 18.75 | I | 300 | 200 | 573 | - | 40 |
| | | II | 573 | 50 | 653 | 60 | |

The samples for measurements No. 1-7 were cut from the same piece of car tyre tread with a size of 5 cm × 3 cm using a punch having an internal diameter of 2.5 mm for smaller samples (measurements No. 1, 3-4, 6-7) or 5.0 mm for larger samples (measurements No. 2 and 5). Such standardization provided similar masses and sizes of the samples within each of the two groups. Minor differences between the samples followed from the deformation of the rubber at the moment of cutting. The samples for the measurements No. 8-10 were not standardized and had an irregular shape.

The measurements No. 1-7 were carried out at a constant heating rate $\beta$ up to the final temperature $T_f$= 1073 K at which the samples were held for 20 minutes. In the measurements No. 8-10 heating of the samples was conducted in two stages at two different heating rates. At the end of the measurements the samples were held at a constant temperature for a specified time (for details see Table 1). The measurements No. 8-10 were used for validation of the kinetic model.

Figure 1 shows a typical course of ELT pyrolysis in a form of the TG and DTG curves. While the TG curve represents the relative sample mass during pyrolysis, the DTG curve (the corresponding first derivative of the TG curve) displays the pyrolysis rate. There are two measurements shown in Fig. 1 (No. 6 and 7). They were carried out at the same heating rate, $\beta$ = 1 K/min. A comparison of the DTG curves demonstrates very high accuracy and repeatability of the measurements. From the modeling point of view, there are also three characteristic maxima indicated on the DTG curves. They correspond to three stages of the process.

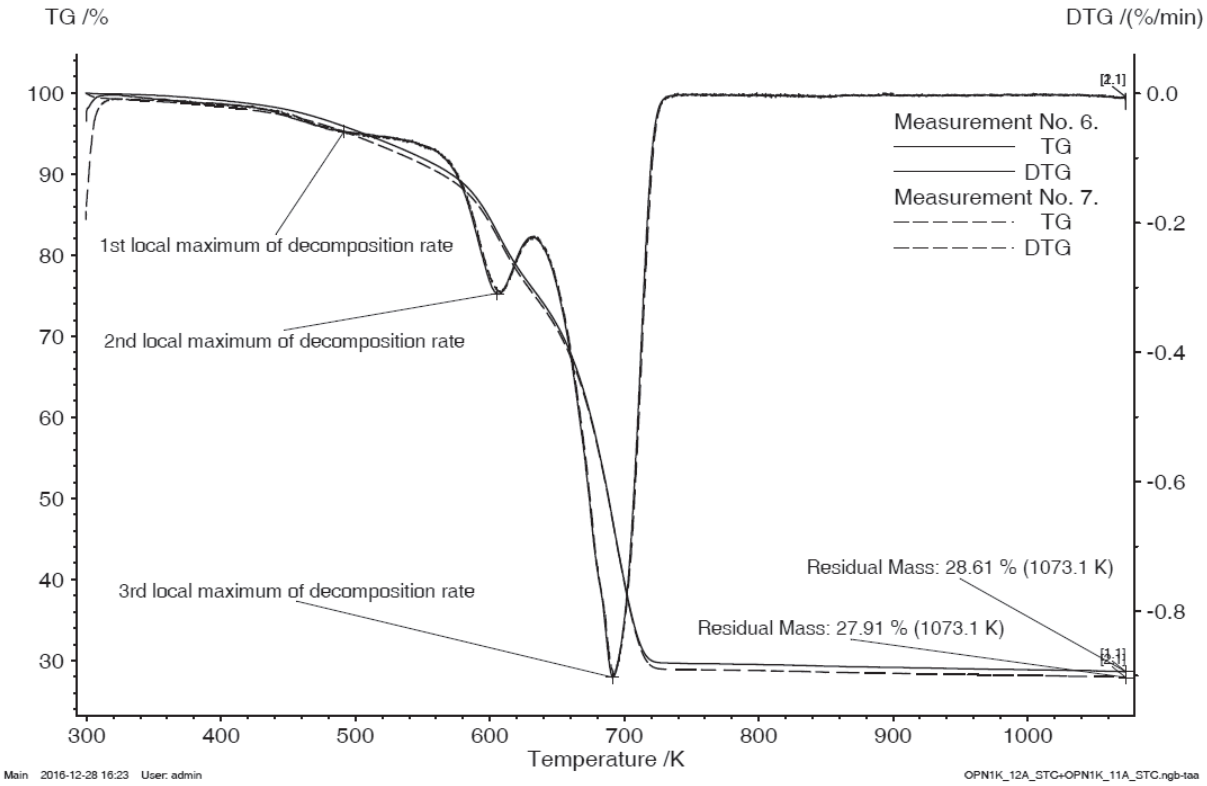


Fig. 1. Comparison of the measurements for heating rate $\beta$ = 1 K/min: TG - relative sample mass, DTG - rate of relative mass loss

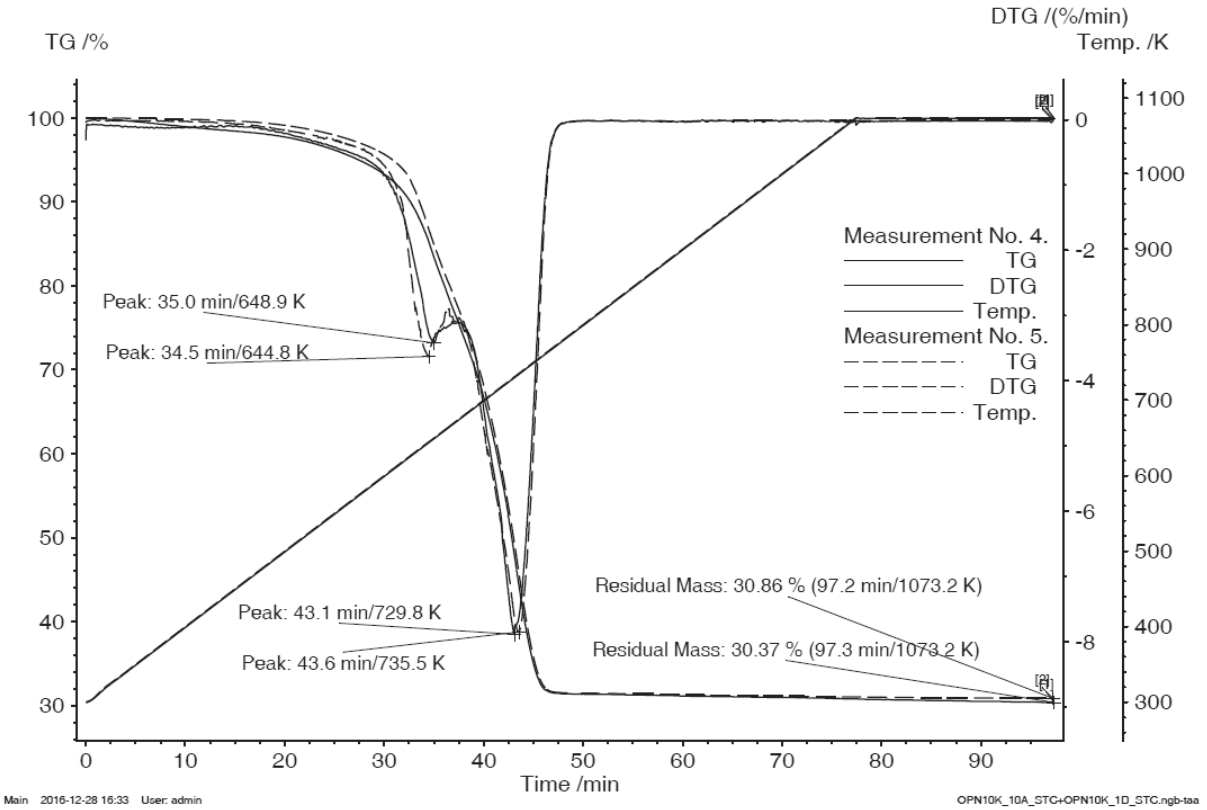


Fig. 2. Comparison of the measurements for heating rate $\beta$ = 10 K/min: TG – relative sample mass, DTG - rate of relative mass loss, Temp. – temperature

The results of two samples with different mass and size (No. 4 and 5) are presented in Fig. 2. The measurements were carried out at the same constant heating rate, $\beta$ = 10 K/min. A comparison of the DTG curves reveals that the differences in the thermal decomposition rates are quite small and consist in a slight shift of maxima on the curves. For the larger of the tested samples (No. 5), the first maximum appears 30 seconds before the corresponding maximum for the smaller sample (No. 4) (34.5 min. / 644.8 K compared to 35.0 min. / 648.9 K). On the other hand, the second maximum appears 30 seconds later than the corresponding maximum for the smaller sample (43.6 min. / 735.5 K compared to 43.1 min./729.8 K). These shifts have the opposite direction, which is probably related to small differences in compositions of the tested samples. This is reflected in the final masses of these samples at the end of pyrolysis (30.86 % compared to 30.37 %).

Similar conclusions can be drawn from a comparison of the DTG curves obtained at the higher heating rate $\beta$ = 50 K/min (Fig. 3). Although both of the compared samples differ significantly in mass and size (No. 1 and 2), the maxima appear at almost identical temperatures. Finally, based on the results shown in Figs. 2 and 3, it can be stated that the conduction resistance did not play a significant role in the milligram scale pyrolysis and it may be omitted from further analysis. Leung and Wang concluded the same on the basis of their experimental results with a granular scrap tyre in four sizes: 1.18 - 2.36 (8 - 16 mesh), 1.0 - 1.18 (16 mesh), 0.5 - 0.6 (30 mesh) and 0.355 - 0.425 mm (40 mesh) (Leung and Wang, 1999). Note that their biggest tyre samples had similar dimensions to our samples from measurements No. 1, 3 - 4, 6 - 7. Similarly, Gonzalez et al. demonstrated that the pyrolysis rate was not affected by the intraparticle and interparticle heat transfer resistances for the particle sizes up to 1.6 mm and the tyre sample masses in the range of 10 - 100 mg, respectively (González et al., 2001). In contradiction with the above findings Lah et al. stated that the internal heat transfer resistance was significant in the tested rubber samples with masses of 7 - 21 mg (Lah et al., 2013). This was deduced from the dynamic TG and DSC runs which present the characteristic shift of the mass loss rate and the generated heat of reaction towards higher temperatures for higher heating rates. Also, Olazar et al. (2005) stated that the heat and mass transfer limitations were significant for tyre particle size between 1.0 and 4.0 mm. This was deduced from the comparison of the kinetic parameters calculated for two particle size ranges (between 0.1 and 0.8 mm and between 0.8 and 4.0 mm) in the range of temperatures between 450 and 600 °C. The kinetic parameters were determined by fitting a first-order rate equation to the experimental results which were obtained from experiments in the conical spouted bed reactor. As follows from the above quoted findings they are clearly contradictory. However, supporting our results, it can be noted that the first two conclusions were drawn directly from the TG measurements with varying sample masses and dimensions while the other findings were deduced indirectly.

Figure 4 shows a comparison of the results obtained for heating rates, $\beta$, in the range of $\beta$ = 1 – 50 K/min. It can be observed from the DTG curves that the process is more rapid when the heating rate increases. Moreover, it is clearly visible that the characteristic maxima of thermal degradation shift towards higher temperatures. This phenomenon has kinetic origin taking into account that the internal heat transfer resistance can be neglected. This aspect will be discussed in the further part of this work.

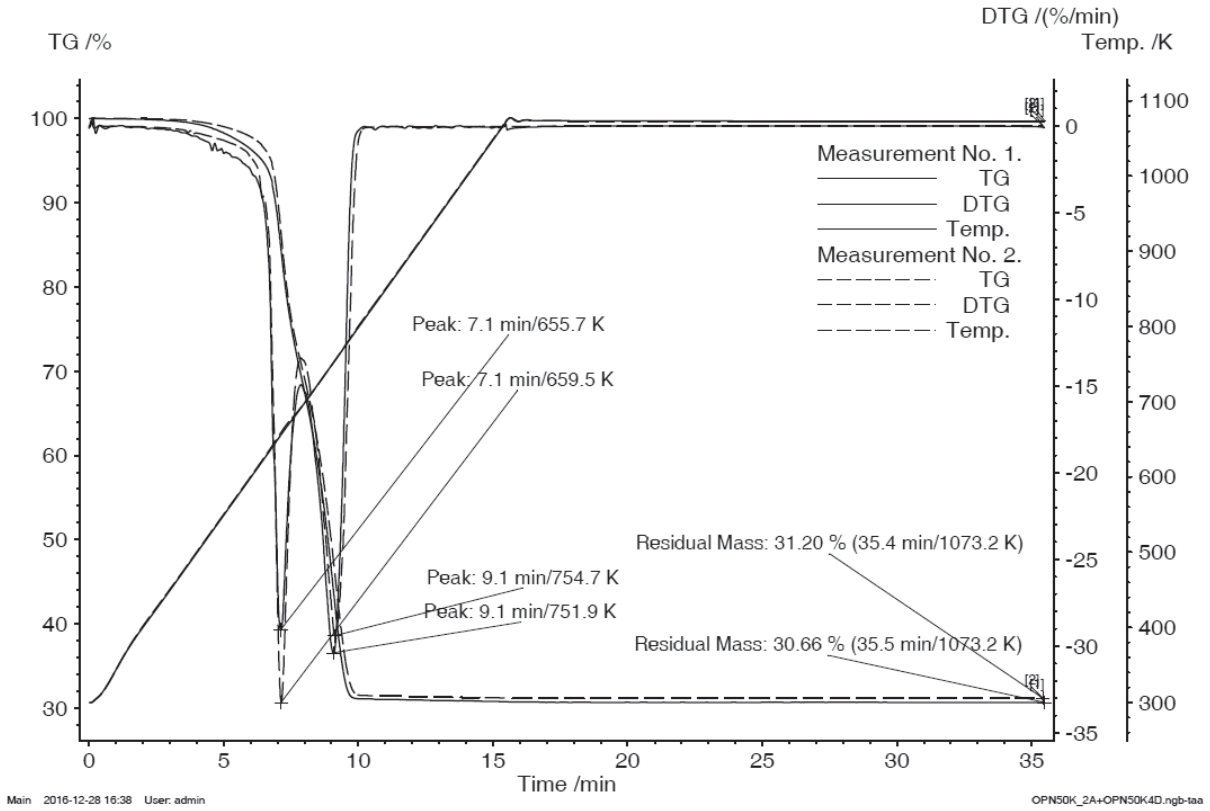


Fig. 3. Comparison of the measurements for heating rate $\beta = 50$ K/min: TG – relative sample mass, DTG - rate of relative mass loss, Temp. – temperature

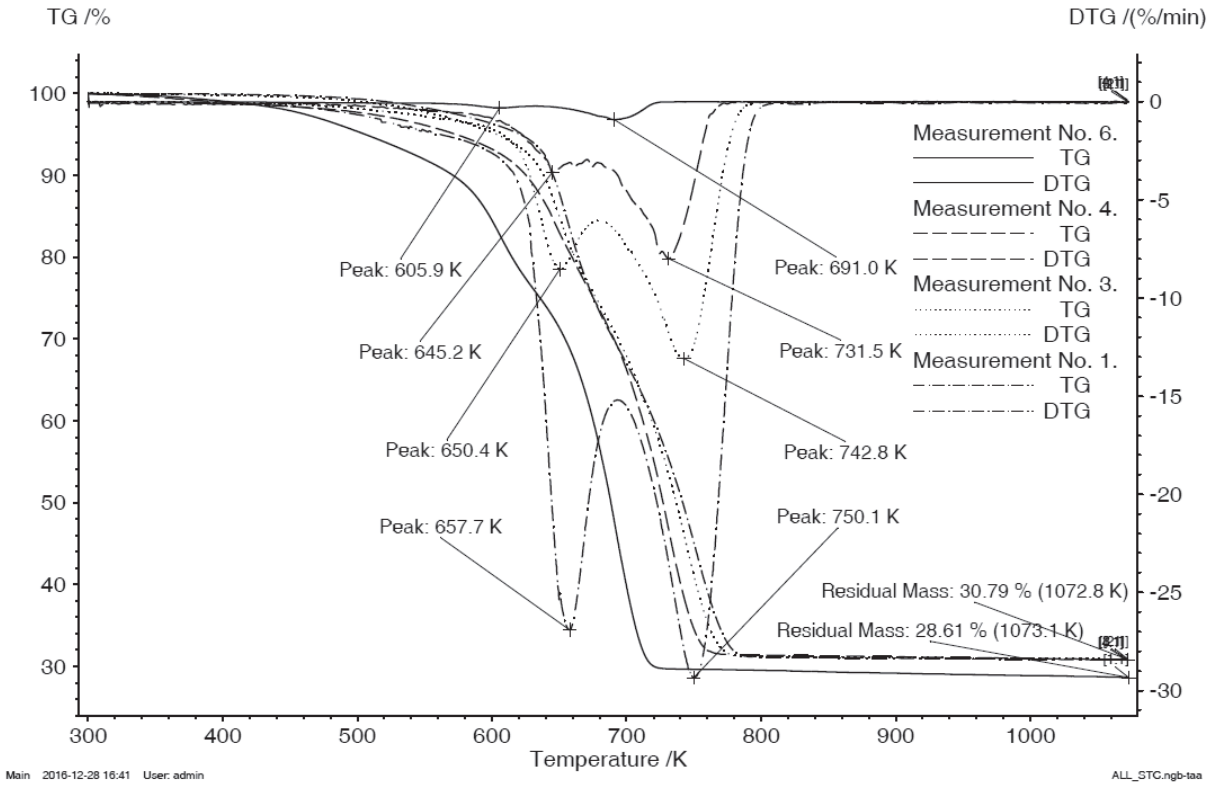


Fig. 4. Comparison of the measurements for different heating rates: TG – relative sample mass, DTG - rate of relative mass loss

## 3. CALCULATIONS

In kinetic modeling of ELT pyrolysis the TCSM was used (Galvagno et al., 2007; Leung and Wang, 1999). This model is based on two key assumptions: (1) car tyres consist of three major components, (2) thermal decomposition of each component takes place independently. Kinetics of the thermal decomposition of the major components is usually modeled as a first- or *n*-order reaction. In this work first-order kinetics was assumed. Therefore, the rate of reaction can be described by the following set of equations:

$$\frac{d\alpha}{dt} = \sum_{i=1}^{3} z_i \frac{d\alpha_i}{dt} \tag{1}$$

and

$$\frac{d\alpha_i}{dt} = A_i e^{-E_i/RT}\left(1-\alpha_i\right) \tag{2}$$

where the conversion of the tyre sample, $\alpha$ is calculated as follows

$$\alpha = \frac{\left(m_0 - m\right)}{\left(m_0 - m_\infty\right)} \tag{3}$$

Because the heating rate was constant in the performed experiments, $\beta = dT / dt$ = const., e.q. (1) can be transformed into an equivalent form (4)

$$\frac{d\alpha}{dT} = \frac{1}{\beta}\sum_{i=1}^{3} z_i \frac{d\alpha_i}{dt} = \sum_{i=1}^{3} z_i \frac{d\alpha_i}{dT} \tag{4}$$

Firstly, to calculate the kinetic parameters the composite function, $d\alpha / dT$ was deconvoluted into three individual thermal decomposition functions describing each of the modeled compounds (Fig. 5). This calculation step was necessary to determine the temperature ranges for the conversions of the three major components. In general, many different peak functions can be used, i.e.: various versions of Gaussian, asymmetric double sigmoidal or log-normal. In this work each thermal decomposition step was modeled using the particular case of extreme function (the Gumbel probability density function distribution) shown below (Galvagno et al., 2007).

$$\frac{d\alpha}{dT} = \sum_{i=1}^{3}\left(\varepsilon_i \exp\left(-\exp\left(-\delta_i\right) - \delta_i + 1\right)\right) \tag{5}$$

where $\delta_i = (T - T_{c,i}) / \omega_{c,i}$ (since the function offset is 0 for the considered case, it is ruled out from this equation).

The Levenberg-Marquardt algorithm was used to compute the following 9 parameters ($i$ = 1, 2, 3): $\varepsilon_i$, $T_{c,i}$ and $\omega_{c,i}$. The calculations consisted in minimizing the sum of squared deviations between the experimental and calculated reaction rates (with Eq. 5), $d\alpha / dT$. Figure 5 shows a comparison of the calculated curve to the experimental one. There are also the thermal decomposition curves for the three major components shown in Figure 5.

The values of $z_i$, denoting the contribution of the *i-th* reaction to the total mass loss, were obtained after integration of the individual decomposition rates giving: $z_1 = 0.0528$, $z_2 = 0.294$ and $z_3 = 0.653$ (see Fig. 6).

Finally, the pre-exponential factor, $A_i$, and the activation energy, $E_i$, were calculated for each major component. The calculations were carried out using the Levenberg-Marquardt algorithm. The aim of the calculations was to minimize the sum of squared deviations between the individual decomposition

rates obtained from deconvolution of the composite function and that calculated from the kinetic model (see Fig. 7).

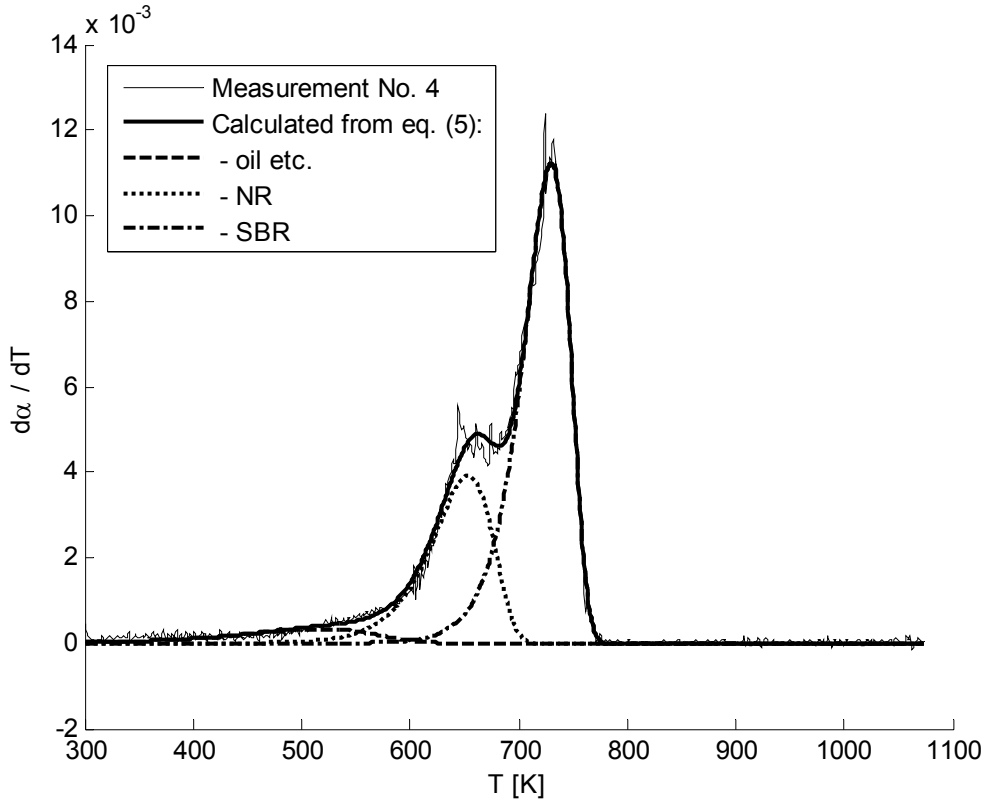


Fig. 5. Comparison of the pyrolysis rate curves: calculated from Eq. (5) and experimental (measurement No. 4), and the decomposition rate curves for three major components (oil etc., NR, SBR)

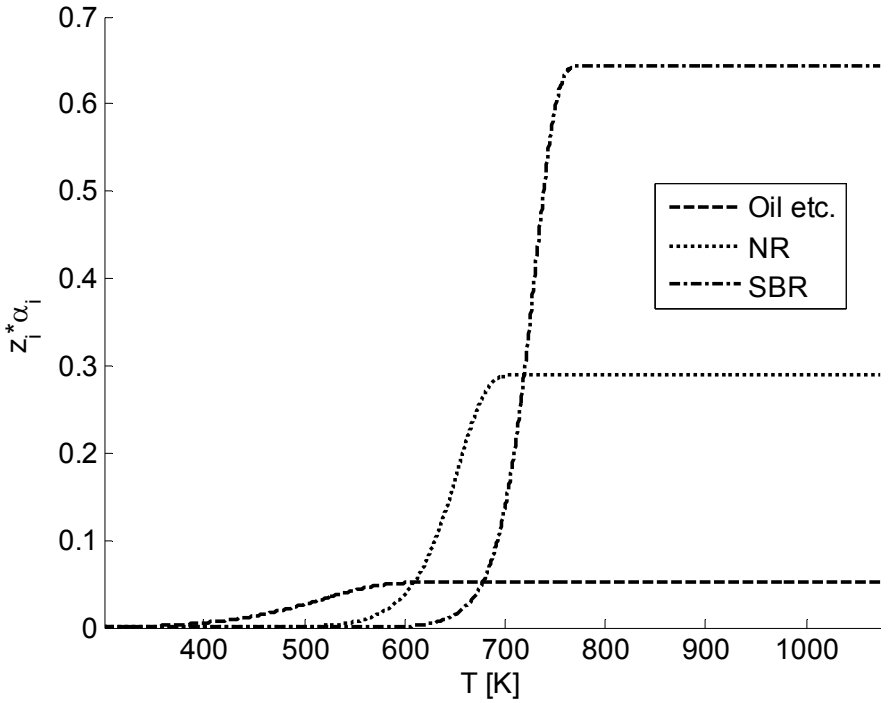


Fig. 6. The integral curves of the decomposition rates for the three major components (oil etc., NR, SBR)

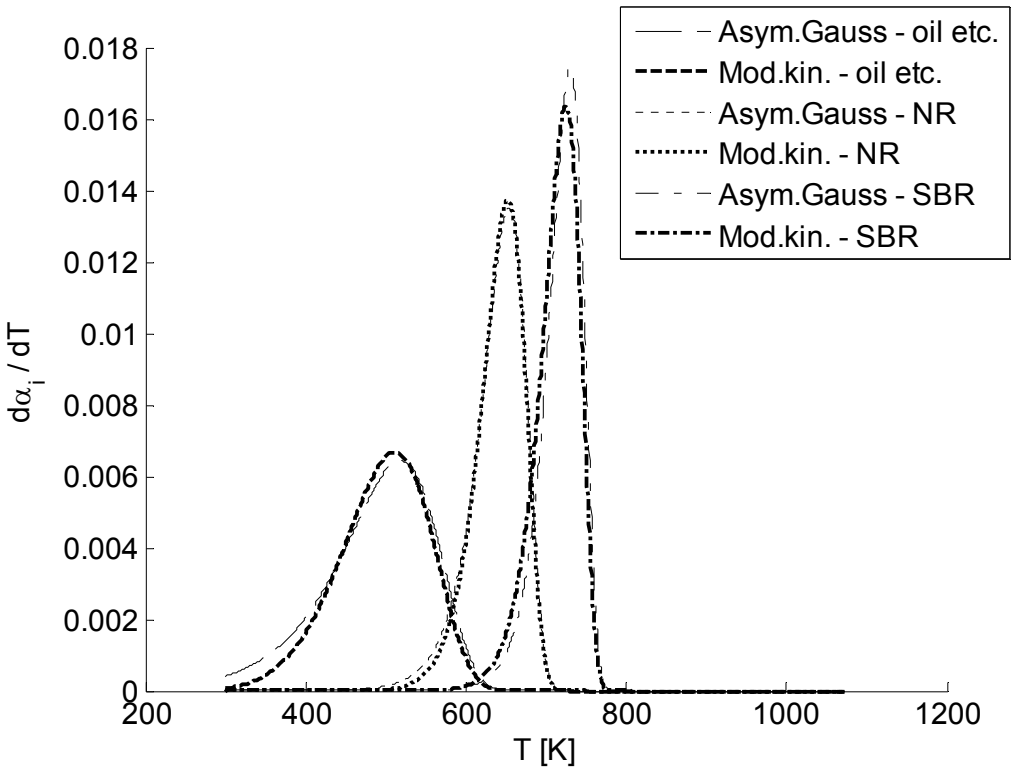


Fig. 7. Comparison of the individual decomposition rates obtained from deconvolution of the composite function and the calculated from the kinetic model

The values of the calculated kinetic parameters are shown in Table 2.

Table 2. Comparison of calculated and literature values of the kinetic parameters

| Component | Heating rate | Kinetic parameters | | Ref. |
|---|---|---|---|---|
| | β (K/min) | *A* (1/min) | *E* (kJ/mol) | |
| 1. Oil etc. | 10 | $3.8\times10^{2}$ | 33.1 | This work |
| | | $2.0\times10^{4}$ | 52.5 | (Leung and Wang, 1999) |
| | | $5.0\times10^{2}$ | 50.3 | (Mui et al., 2010) |
| | | $9.34\times10^{2}$ | 38.7 | (Kim et al., 1995) |
| | | $1.00\times10^{5}$ | 66.8 | (González et al., 2001) |
| 2. NR | | $3.1\times10^{9}$ | 124.1 | This work |
| | | $6.3\times10^{13}$ | 164.5 | (Leung and Wang, 1999) |
| | | $1.9\times10^{7}$ | 102.8 | (Mui et al., 2010) |
| | | $3.78\times10^{16}$ | 209.0 | (Kim et al., 1995) |
| | | $3.00\text{x}10^{4}$ | 44.8 | (González et al., 2001) |
| 3. SBR/BR | | $1.6\times10^{11}$ | 161.6 | This work |
| | | $2.3\times10^{9}$ | 136.1 | (Leung and Wang, 1999) |
| | | $1.13\times10^{17}$ | 237.1 | (Mui et al., 2010) |
| | | $8.75\times10^{8}$ | 127.3 | (Kim et al., 1995) |
| | | $7.56\times10^{2}$ | 32.9 | (González et al., 2001) |

Note that there is no relationship between the parameters of the auxiliary model presented in Eq. (5) and the kinetic parameters presented in Table 2. As noted earlier, the auxiliary model (5) was only needed to deconvolute the composite function $d\alpha / dT$ obtained from TGA.Significant differences in the values of kinetic parameters can be seen in Table 2. This possibly results from different composition of the tyres used in these individual experiments. To some extent, this effect was also visible in our measurements. This is indicated by the residual mass after pyrolysis which varies in successive experiments (see Fig. 4). Although the reported differences are not very pronounced, one should note that the samples for the analysis were taken from the same piece of tyre with a size of 5 cm × 3 cm. In the case of different brands and/or pieces of tyres this effect can be naturally enhanced. The kinetic parameters calculated in this work for NR and SBR/BR are in the range of reported values by other authors. On the other hand, the parameters obtained for the first component (oil etc.) are beyond the range. However, given that this modeling component comprises not only the processing oil but also plasticizer, moisture and other specific additives, the values of its kinetic parameters depend on the composition of the tyre and the initial moisture content, which can vary for different tyre samples.

The conversion vs. temperature curve was obtained by integration of the kinetic model. Figure 8 shows a comparison of the calculated and experimental profiles for measurement no. 4. A quite accurate prediction is observed. This is because the kinetic parameters were determined from the same measurement. More validation cases are presented in Figs. 10 - 13.

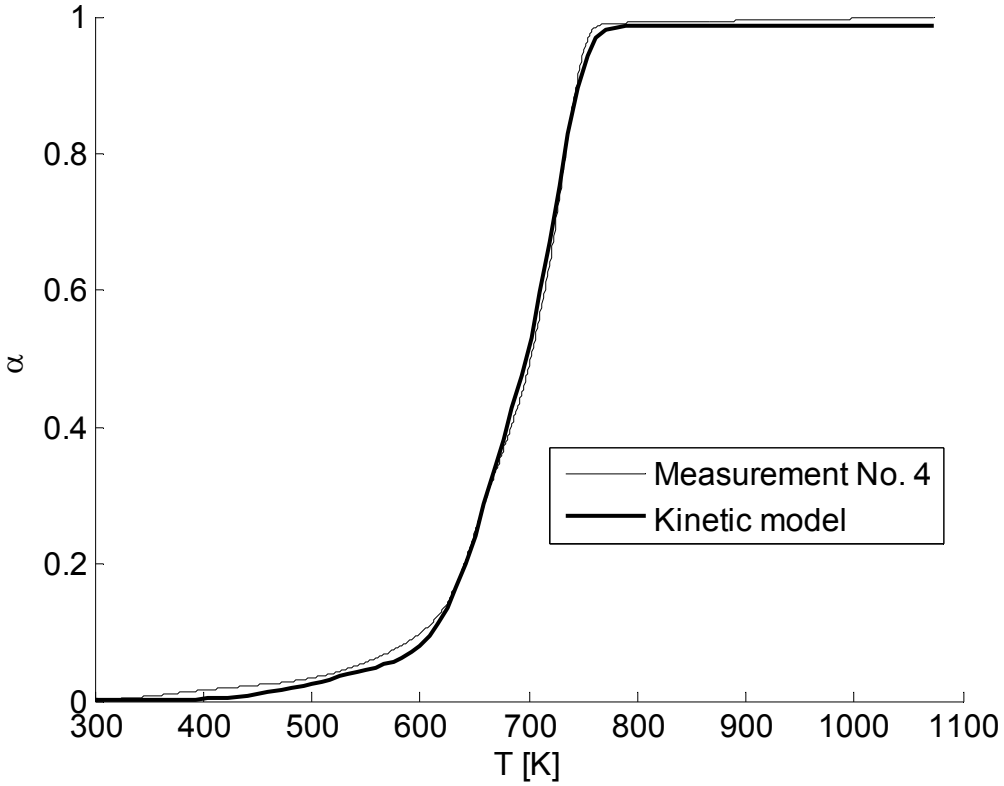


Fig. 8. Comparison of the conversion curves: calculated form the kinetic model and experimental (measurement No. 4)

Figure 9 shows the results of integration of the kinetic model for different heating rates in the range of 1 - 50 K/min. The temperatures corresponding to the conversion of 0.5 are also indicated in Figure 9 for each of the calculated curves.

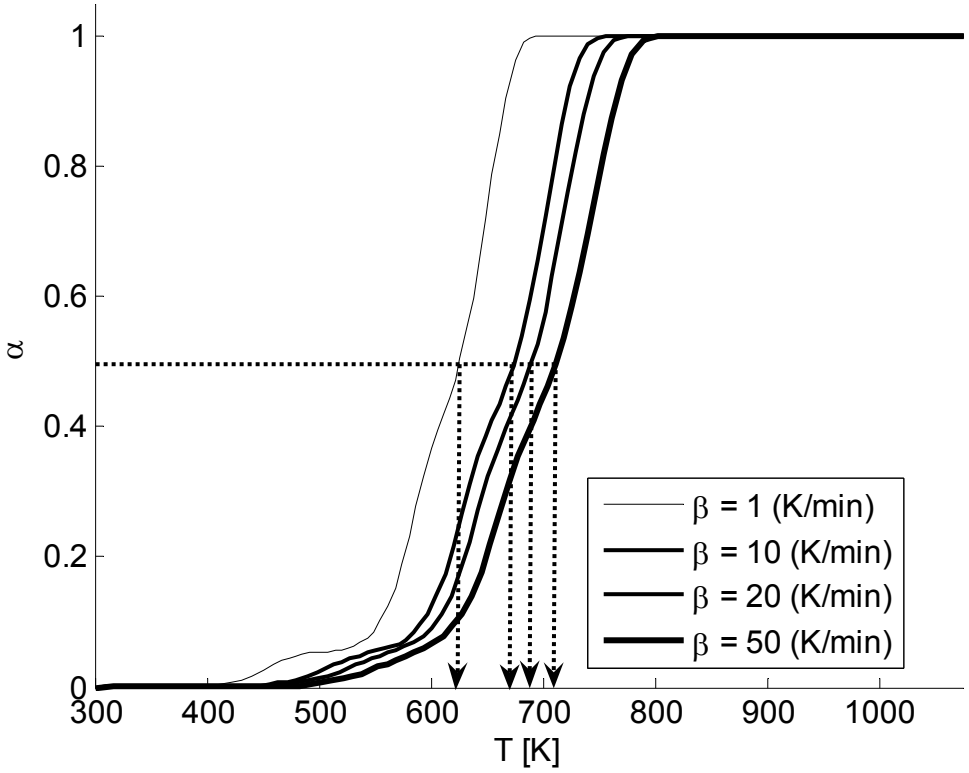


Fig. 9. Effect of heating rate, $\beta$, on the conversion curves, $\alpha$, as predicted by the kinetic model

The most remarkable result to emerge from the data is that the calculated results explain the phenomenon of shifting the characteristic maxima on the DTG curve in the direction of higher temperatures for higher heating rates. The phenomenon is observed in this work (see Fig. 4) and many previous publications (Galvano et al., 2007; González et al., 2001; Lah et al., 2013; Leung and Wang, 1999; Mui et al., 2010; Seidelt et al., 2006). Intuitively, this can be related to the internal heat transfer resistance. But given that the conduction resistance is negligible in the tested milligram samples, as shown in the previous part of this work, it is evident that the phenomenon is caused by the kinetics itself. Thus, this effect is caused by the different residence times of the samples in the varying temperature (sample history). As can be seen from the experimental results in Fig. 4 and from the modeling results in Fig. 9, the tested milligram tyre sample needs longer time when the heating rate is higher to reach a certain level of conversion.

Testing of the kinetic model was carried out using the experiments No. 8 - 10 (see Table 1). As mentioned earlier these experiments were performed for variable heating rates. A comparison of the experimental and calculated results is shown in Figs. 10 - 12.

The kinetic model predicts the first two experiments correctly (Figs. 10 and 11). On the other hand, the quality of prediction for the third experiment is worse with a maximum error of 20% (Fig. 12). A comparison of the conditions under which these experiments were conducted showed that the experiment No. 10 was performed at the highest heating rates (1st stage $\beta = 200$ K/min / 2nd stage $\beta = 50$ K/min). Therefore, another test was conducted, in which the same kinetic model was used. However, this time, the kinetic parameters were determined from the measurement No. 1 in which the heating rate was $\beta = 50$ K/min. Then, the kinetic model was tested again by comparison of the calculated results to the experimental results. This time, it turned out that the model predicted the experiment very well (Fig. 13).

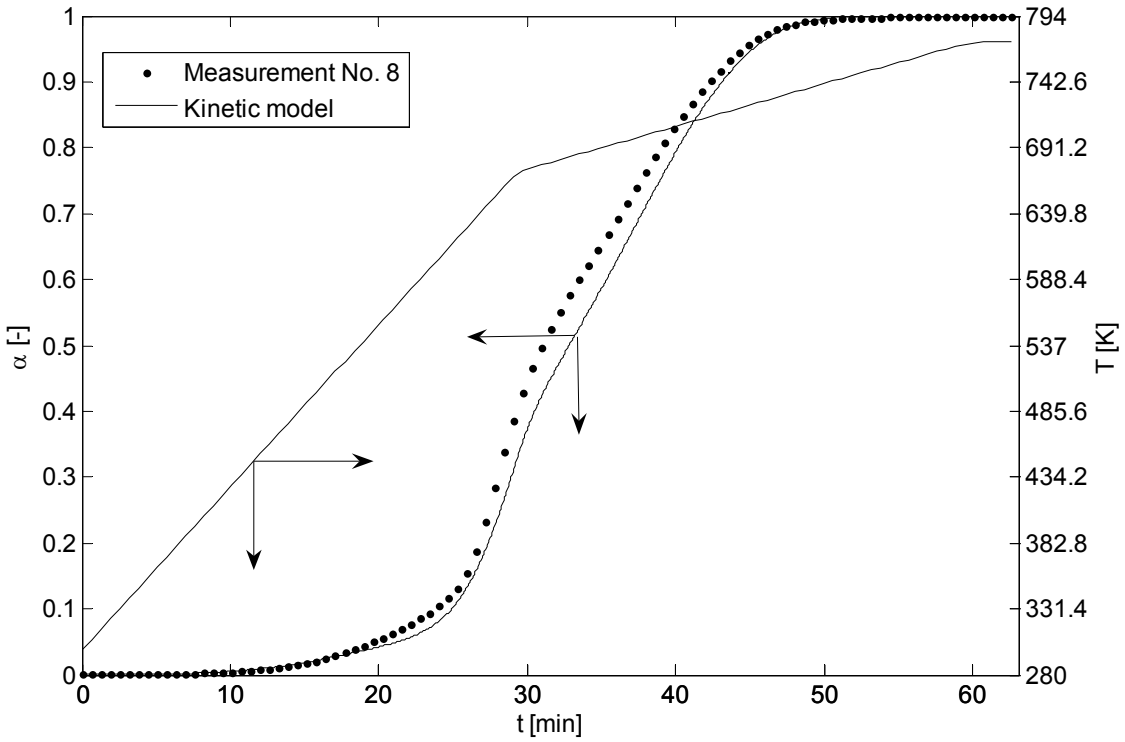


Fig. 10. Testing of the kinetic model based on measurement No. 8

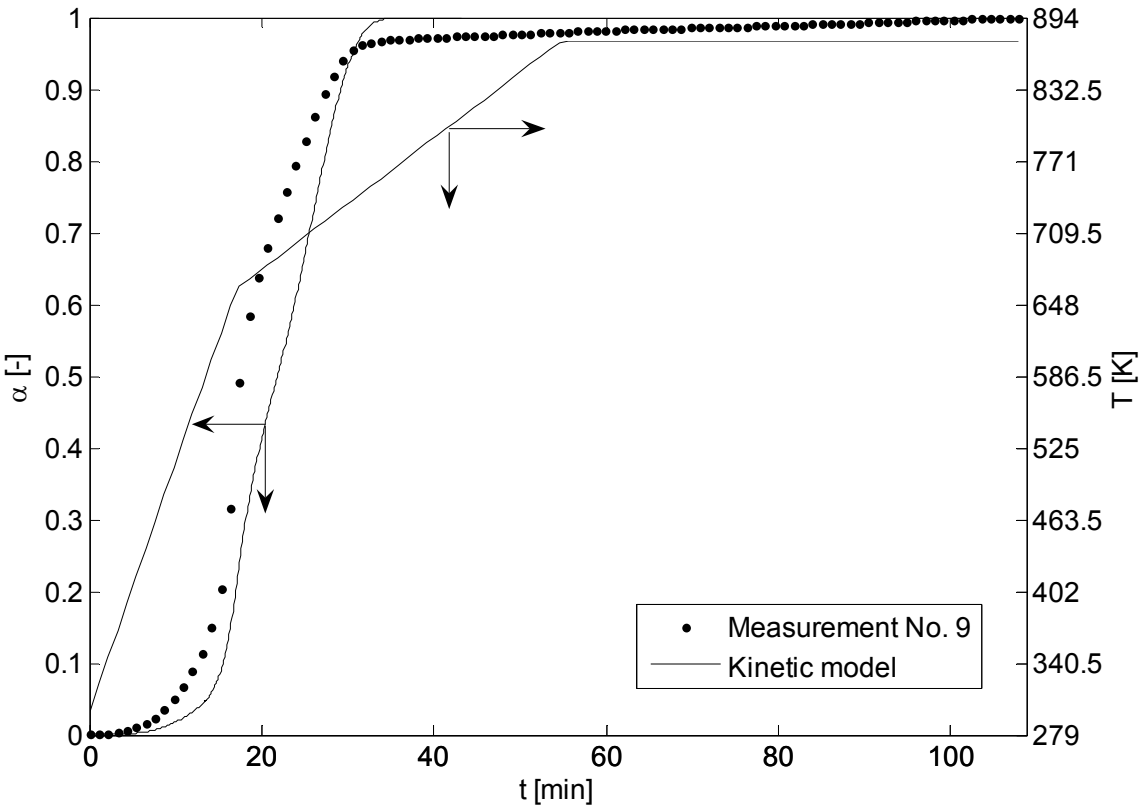


Fig. 11. Testing of the kinetic model based on measurement No. 9

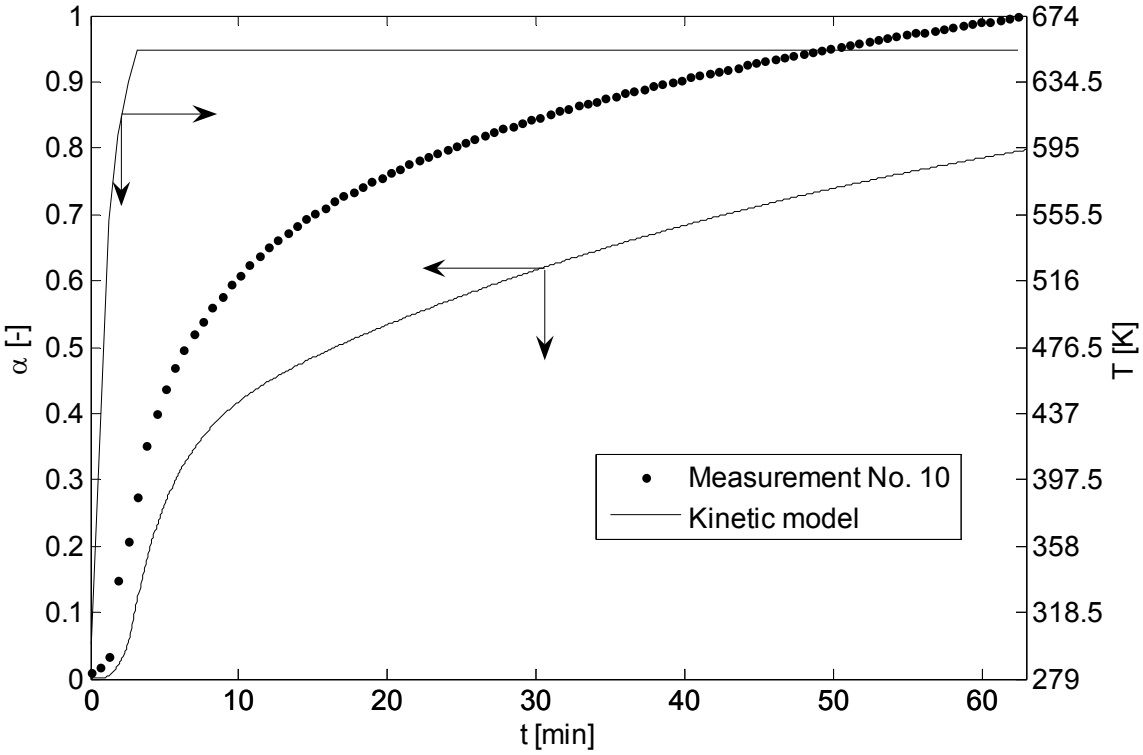


Fig. 12. Testing of the kinetic model based on measurement No. 10

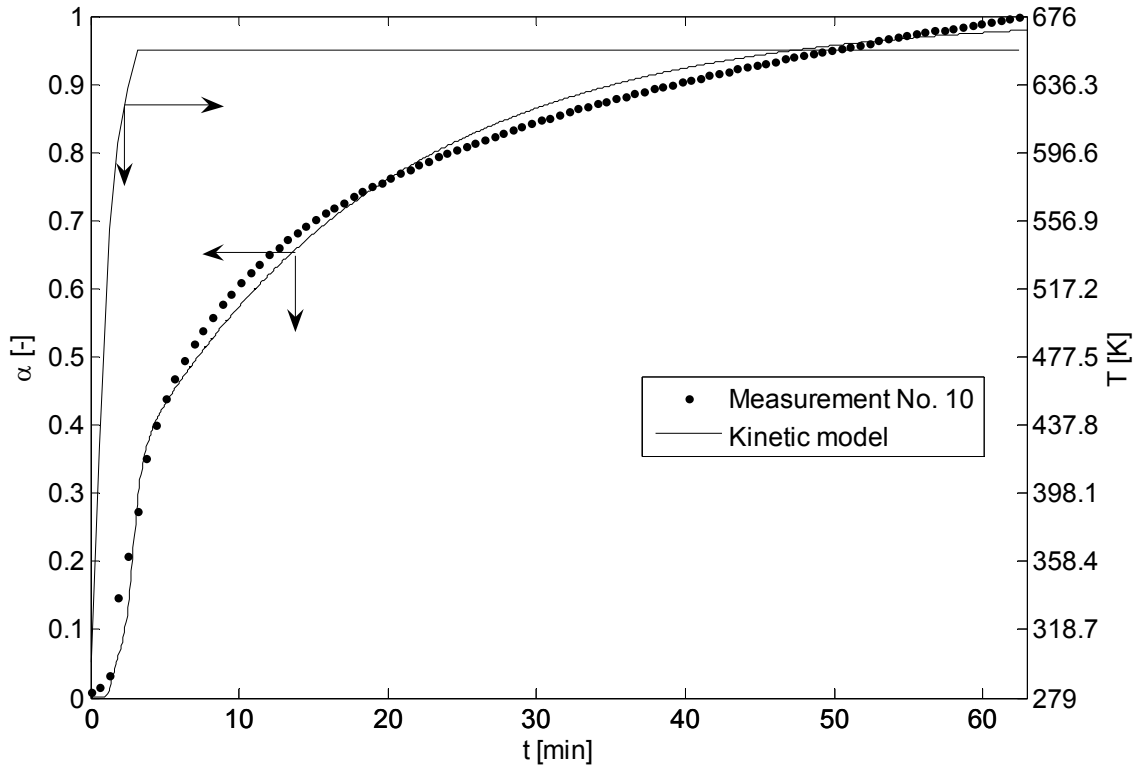


Fig. 13. Testing of the kinetic model based on measurement No. 10. The kinetic parameters were calculated from the measurement No. 1 conducted at heating rate $\beta = 50$ K/min

## 4. CONCLUSIONS

- The measurements showed that three characteristic steps can be distinguished in ELT pyrolysis. These steps correspond to the evaporation and thermal decomposition of: 1) oil, plasticizer, additives and moisture in the first step, 2) natural rubber in the second step, and 3) styrene-butadiene rubber in the third step.
- The Three-Component Simulation Model was able to correctly describe the kinetics of ELT pyrolysis. However, the accuracy of predictions was enhanced if the parameters of the kinetic model were determined from the measurement carried out at a similar heating rate.
- Comparison of DTG curves for samples of different sizes showed that the conduction resistance in the samples was negligible. This enabled detailed kinetic analysis of ELT pyrolysis by TG analysis.
- The calculation results obtained for different heating rates explain the cause of the observed shifting of the local maxima on the DTG curves in the direction of higher temperatures for higher heating rates. This work shows that the phenomenon has kinetic origin and follows directly from different residence times of samples at varying temperatures (history of the sample).
- CFD modeling of pyrolysis reactors requires a reliable and computationally cheap kinetic model. The Three-Component Simulation Model due to its relative simplicity seems to be an appropriate candidate for this.

*The project funded by the National Centre for Research and Development and the European Union under the European Regional Development Fund under the agreement UOD-DEM-1-217 / 001.*

## SYMBOLS

| | |
|---|---|
| $A$ | pre-exponential factor, 1/min |
| $c_p$ | heat capacity, J/(kg·K) |
| $DTG$ | rate of relative mass loss, %/min |
| $E$ | activation energy, kJ/mol |
| $m$ | sample mass, mg |
| $T$ | temperature, K |
| $T_c$ | parameter of the extreme function |
| $t_{isotherm.}$ | length of the isothermal stage, min |
| $Temp$ | temperature, K |
| $TG$ | relative sample mass, % |
| $\dot{V}$ | flow rate, ml/min |
| $z_i$ | contribution of the *i-th* reaction to the total mass loss |

*Greek symbols*

| | |
|---|---|
| $\alpha$ | conversion |
| $\beta$ | heating rate, K/min |
| $\delta_i = (T - T_{c,i}) / \omega_{c,i}$ | parameter of the extreme function for the i-th component |
| $\varepsilon_i$ | parameter of the extreme function for the i-th component |
| $\omega_{c,i}$ | parameter of the extreme function for the i-th component |

*Subscripts*

| | |
|---|---|
| $0$ | initial |

| | |
|---|---|
| $f, \infty$ | final |
| $i$ | *i-th* component |
| $N_2$ | nitrogen |

## REFERENCES


Al-Salem S.M., Lettieri P., Baeyens J., 2009. Kinetics and product distribution of end of life tires (ELTs) pyrolysis: a novel approach in polyisoprene and SBR thermal cracking. *J. Hazard. Mater.*, 172, 1690–1694. DOI: 10.1016/j.jhazmat.2009.07.127.

Chen J.H., Chen K.S., Tong L.Y., 2001. On the pyrolysis kinetics of scrap automotive tires. *J. Hazard. Mater.*, 84, 43-55. DOI: 10.1016/S0304-3894(01)00180-7.

Council Directive 1999/31/EC of 26 April 1999 on the Landfill of Waste. 1999. Office for Official Publications of the European Communities Luxembourg.

Council Directive 91/156/EEC of 18 March 1991 Amending Directive 75/442/EEC on Waste. 1991. Council of European Communities. European Commission: Brussels.

ETRMA's End-of-life Tyres Management report, 2015. Available at: http://www.etrma.org/tyres/ELTs.

Galvagno S., Casu S., Martino M., Di Palma E., Portofino S., 2007. Thermal and kinetic study of tyre waste pyrolysis via TG-FTIR-MS analysis. *J. Therm. Anal. Calorim.*, 88, 507-514. DOI: 10.1007/s10973-006-8409-1.

González J.F., Encinar J.M., Canito J.L., Rodríguez J.J., 2001. Pyrolysis of automobile tyre waste. Influence of operating variables and kinetics study. *J. Anal. Appl. Pyrolysis*, 58, 667-683. DOI: 10.1016/S0165-2370(00)00201-1.

Islam M.R., Haniu H., Fardoushi J., 2009. Pyrolysis kinetics behavior of solid tire wastes available in Bangladesh. *Waste Manage.*, 29, 668-677. DOI: 10.1016/j.wasman.2008.04.009.

Kim S., Park J., Chun H., 1995. Pyrolysis kinetics of scrap tire rubbers. I: Using DTG and TGA. *J. Environ. Eng.*, 121, 507-514. DOI: 10.1061/(ASCE)0733-9372(1995)121:7(507).

Lah B., Klinar D., Likozar B., 2013. Pyrolysis of natural, butadiene, styrene-butadiene rubber and tyre components: Modelling kinetics and transport phenomena at different heating rates and formulations. *Chem. Eng. Sci.*, 87, 1-13. DOI: 10.1016/j.ces.2012.10.003.

Leung D.Y.C., Wang C.L., 1999. Kinetic modeling of scrap tire pyrolysis. *Energy Fuels*, 13, 421-427. DOI: 10.1021/ef980124l.

Mui E.L.K., Cheung W.H., Lee V.K. C., McKay G., 2010. Compensation effect during the pyrolysis of tyres and bamboo. *Waste Manage.*, 30, 821-830. DOI: 10.1016/j.wasman.2010.01.014.

Mui E.L.K., Lee V.K.C., Cheung W.H., McKay G., 2008. Kinetic modeling of waste tire carbonization. *Energy Fuels*, 22, 1650-1657. DOI: 10.1021/ef700601g.

Quek A., Balasubramanian R., 2009. An algorithm for the kinetics of tire pyrolysis under different heating rates. *J. Hazard. Mater.*, 166, 126-132. DOI: 10.1016/j.jhazmat.2008.11.034.

Quek A., Balasubramanian R., 2012. Mathematical modeling of rubber tire pyrolysis. *J. Anal. Appl. Pyrolysis*, 95, 1-13. DOI: 10.1016/j.jaap.2012.01.012.

Rudniak L., Machniewski P., 2017. Modelling and experimental investigation of waste tyre pyrolysis process in a laboratory reactor. *Chem. Process Eng.*, 38, 445-454. DOI: 10.1515/cpe-2017-0034.

Seidelt S., Müller-Hagedorn M., Bockhorn H., 2006. Description of tire pyrolysis by thermal degradation behaviour of main components. *J. Anal. Appl. Pyrolysis*, 75(1), 11-18. DOI: 10.1016/j.jaap.2005.03.002.

Williams P.T., 2013. Pyrolysis of waste tyres: A review. *Waste Manage.*, 33, 1714-1728. DOI: 10.1016/j.wasman.2013.05.003.


*Received 26 October 2016*
*Received in revised form 12 June 2017*
*Accepted 17 June 2017*